IAC-10-A6.5.5

PRELIMINARY TELESCOPE DESIGN ANALYSIS FOR THE OPTICAL SPACE SURVEILLANCE SUBSYSTEM

A. Vananti
Astronomical Institute University of Bern (AIUB), Bern, Switzerland, alessandro.vananti@aiub.unibe.ch

T. Schildknecht
Astronomical Institute University of Bern (AIUB), Bern, Switzerland, thomas.schildknecht@aiub.unibe.ch

P. Keinänen
ASRO, Turku, Finland, perkeina@utu.fi

J. Kuusela
ASRO, Turku, Finland, jyri.kuusela@asro-space.com

H. Krag
European Space Operations Centre (ESOC), Darmstadt, Germany, holger.krag@esa.int

ABSTRACT

The European Space Agency (ESA) is developing an independent system for Space Situational Awareness (SSA). One component of the draft architecture of the system foresees a network of optical telescopes for observations in the MEO/HEO/GEO region. The telescope network will survey and track all objects above a certain diameter and will deliver data to allow the collection of accurate orbits and possibly information on the object properties. Major design drivers are the requirements on the limiting object size, the timeliness for particular events such as fragmentations or maneuvers, and the orbit accuracy for cataloguing. For the optical sensors these requirements translate into wide FOV's and large apertures. In this work, different design options for the optical telescope assembly are evaluated and a trade-off analysis in terms of capability and costs is given. The identification of key telescope parameters according to the required sensitivity and tracking requirements is discussed. Among the various design aspects, especially the trade-off's between aperture and focal ratio, FOV and detector size, as well as pixel size and readout time are treated. As a result of the analysis a possible telescope design for the SSA optical network is presented.

INTRODUCTION

In this article the optimal telescope design parameters for the optical part of a future European Space Situational Awareness (SSA) system, in terms of system performance, requirements compliance, and costs are evaluated. The key telescope parameters are identified and assessed against the given SSA requirements. Based on this analysis a preliminary list of design requirements is consolidated. Different design options with different key parameters are considered: some design might be better for certain purposes, whereas other might have interesting features like simplicity and low development cost. It is important to estimate these values for a wide range of design options so that during a later phase it is possible to select designs which best fit the overall performance of the system.

For the proposed surveillance system, depending on the number and size of the search fields, different field of view (FOV) values might be required to ensure a certain re-observation frequency. On the other hand, the aperture diameter of the telescope determines the limiting object detection size, the limiting signal-to-noise ratio (SNR), and the exposure time. The Space Surveillance Network (SSN) telescope preferably should have a very large FOV and a large aperture, but these two requirements are in conflict and it is very difficult to have a reasonable compromise between them. One of the constraints limiting the SNR is the background light. The contributions to the background are the sky background, stray light, dark current from the sensor, and various noise contributions in the amplified detector output.

In the choice of the camera different factors need to be considered. Charge-Coupled Devices (CCD's) are known technology and produce good image quality with very low readout noise and high sensitivity. For astronomical imaging applications they are usually the preferred sensors. However the readout time is rather long, which doesn't fit well to the current application and longer gaps between the exposures or higher readout noise have to be accepted. The data transfer out from sensor produces a bottle neck, where low noise

requires reasonable integration time for each pixel. On the other hand if the device is a mosaic or has more readout channels, better readout times can be achieved. Additional to the sensor, control electronics is needed, together with low noise levels, which are required for high quality astronomical cameras. Since the dark current in all above sensors is significant, in order to be able to take several seconds exposures from faint objects, the sensor has to be cooled.

The mechanical design of the telescope is another important component: the telescope should be able to quickly change its pointing direction and to stabilize in order to take the next exposure. During this time the image is read out from the camera. In principle, it is not impossible to turn the telescope by few degrees within few seconds, but the final pointing has to be reached within an accuracy of arcseconds, which is a very demanding requirement. Short tube length and lightweight structures improves the stabilization time, yet making the design more complex and more expensive.

ANALYSIS OF TELESCOPE COMPONENTS

Optical telescope assembly

The first telescope component to analyze is the Optical Telescope Assembly (OTA) which is defined to include the primary mirror, secondary mirror and their related support structure. Different existing telescopes were examined to appraise the technology constraints in the current optical systems. A representative of the most interesting telescopes with wide-field capabilities is shown in Table 1. Some of the professional telescopes come close to serious amateur telescopes in regard to some parameters (TAROT, ROSACE) and the analysis of interesting projects, like e.g. the Bradford telescope, gives indications about the potential of totally Commercial Off-The-Shelf (COTS) constructed systems with essentially smaller related costs. The following telescopes are considered:

- Panoramic Survey Telescope and Rapid Response System (Pan-STARRS, under construction) [RD-1],
- Large Synoptic Survey Telescope (LSST, under construction) [RD-2],
- Catalina Sky Survey Schmidt (CSS S) telescope (Mt. Bigelow, AZ) [RD-3],
- Siding Spring Uppsala Schmidt (SSS S) telescope (Siding Spring Ob., AU) [RD-4],
- Siding Spring 40-inch telescope (SS 40-inch, Siding Spring Ob., AU) [RD-5],
- Mount Lemmon Survey (MLS C) telescope (Mt. Lemmon, AZ) [RD-6],
- Restitution d'Orbite par Système Autonome CCD d'Ecartométrie (ROSACE, Meudon, FR) [RD-7],
- Michigan Orbital Debris Survey Telescope (MODEST, Cerro Tololo, CL) [RD-8],
- Sloan Digital Sky Survey (SDSS) telescope (Apache Point Ob., NM) [RD-9],
- Télescope à Action Rapide pour les Objets Transitoires (TAROT, Plateau de Calern, FR, and La Silla Ob., CL) [RD-10],
- Passive Imaging Metric Sensor (PIMS) (Herstmonceux, UK, Gibraltar, and Cyprus) [RD-11],
- Zimmerwald Laser and Astrometric Telescope (ZIMLAT, Zimmerwald, CH) [RD-12],
- ESA Space Debris Telescope (ESASDT, Tenerife, ES) [RD-13],
- Bradford robotic telescope (Tenerife, ES) [RD-14].

Name	D [m]	F []	f [m]	FOV [°]	Type
Pan-STARRS	1.9	4.3	8	3	RC
LSST	8.4	1.25	10.5	3	P
CSS S	0.68	1.9	1.3	2.8	S
SSS S	0.52	3.4	1.75	2.05	S
SS 40-inch	1	8	8.1	0.35	RC
MLS C	1.5	2	3	1.1	C
ROSACE	0.5	3.8	1.9	0.4	N
MODEST	0.6	3.5	2.1	1.3	S
SDSS	2.5	5	12.5	3	RC
TAROT	0.25	3.5	0.9	1.9	N
PIMS	0.4	10	4.1	0.6	SC
ZIMLAT	1	10	10.3	0.2	RC
ESASDT	1	4.4	4.5	0.7	RC
Bradford	0.36	11	4.0	0.4	SC

Table 1. Primary mirror diameter (D), focal ratio (F), focal length (f), and FOV of different telescopes. The types are: Newton (N), Schmidt (S), Cassegrain (C), Schmidt-Cassegrain (SC), Ritchey-Chretien (RC), Paul (P).

The data show that most of the telescopes hardly reach wide FOV for large apertures. The CSS and SSS telescopes reach more than 2 deg FOV, both with a Schmidt design and relative small apertures of 0.68 m and 0.52 m. Without a Schmidt corrector the covered FOV and the aperture diameter are even smaller, as for the TAROT telescope, with 1.9 deg FOV but an aperture of only 0.25 m. Very few big and expensive projects like the Pan-STARRS, LSST, and SDSS telescopes attain 3 deg FOV with impressive large apertures.

In general, the limitation in FOV and usable image plane width is set by vignetting and aberrations which are always present in real telescope systems. Aberrations tend to increase moving away from the optical axis, thus there is a certain limit in the usable image plane without additional correction optics.

Additional optics tends to increase other image distortions, like chromatic aberration, and to lose light due to reflections at surfaces and absorption in the lens material. The field curvature of the image plane needs to be corrected with specific field flatteners. The manufacture of large aspherical optical components is an additional challenge. Novel polishing techniques, like Magneto-Rheological Finishing (MRF) or ion-beam polishing can produce very complex aspherical surfaces with large aspherical deviations. The limiting factors are the extent of the surface variations and the size of the elements that the machine can process. MRF machines can handle objects which are less than half a meter in diameter, ion beam polishers need vacuum chambers with a maximal size of about two meters at the moment. The working contact area with MRF is in the submillimeter and with ion-beam polishers in the millimeter range. With classical lapping machines the minimum tool width is in the centimeter range. These factors set the limit for the aspherical shape changes on the surface. The shape can not change too much under the tool contact, otherwise the latter does not work in a controllable manner. The surface shape under the tool footprint must be close to spherical.

To reach large FOVs are usually complicated designs necessary. Multi-mirror designs are considered to be suitable only for very large telescopes, where the loss of light due to the additional mirror surfaces is tolerated. Although the gravity does not affect as strongly the Schmidt corrector as large lenses, generally, the Schmidt telescopes, with a long structure and high rotational inertia, are inconvenient for space observations which need short exposures and swift repositioning, as in the frame of SSA.

An analysis of different optical design concepts shows that the topic has still potential for further development. New technologies allow better mirror or lens manufacturing and computers allow more sophisticated ray-trace simulations for more complex optical systems. Wide FOV's can be obtained with optical correctors producing higher quality images with lower distortions. Ackermann et al. [RD-15] refers to a five lens, spherical refractive corrector able to extend the FOV of a telescope with Ritchey-Chrétien design and 1.25 m aperture up to 4.25 deg. McGraw and Ackermann [RD-16] analyze different designs with one-, two-, three-, and four-mirror approaches and different optical correctors. The most promising designs base on field-corrected RC or super-RC systems, but also one-mirror solutions with 6 spherical lenses are presented. All the designs reach 4 deg FOV or more with 1.2 m aperture diameter.

Camera

CCDs are the choice of most astronomers in the near-UV to near-IR band. The absorption length of light in silicon changes from 10 nm to 0.1 mm at wavelengths from 350 nm to 950 nm. Because of the effective absorption, silicon detectors are not well suited for UV measurements. Any structure in front of the detector or dead layer in back of the detector will prevent photon detection. The contrary takes place near IR. Red photons travel deep into the silicon before absorption. Thick active layers are needed near infrared, and at 1100 nm silicon becomes nearly transparent. The CCDs for astronomy are generally back-side illuminated. Quantum efficiency (QE), the charge produced by one photon, of the back illuminated thick CCDs can be high outperforming most other detectors. Special antireflective coatings can be used for improving the detector performance at certain wavelengths. Modern CCD chips are manufactured in many formats: there is a large selection of different pixel formats, and several other options to choose from, including focussing micro-lenses, special coatings and advanced packaging. Very large chips, with >4k x 4k pixels, are emerging from the chip foundries to commercial market. Typical features can include Multi Phased Pinned (MPP), or inverted operation for reduction of the dark current. Antiblooming (pixel charge overflow) circuitry can be also included in the detector structure, but is typically not part of the detectors used in astronomy.

Cooling the CCD reduces dark current to negligible levels, allowing exposure times of up to hours in duration. To achieve the highest possible sensitivity, astronomers cool the CCD usually with liquid nitrogen. MPP or inverted operation reduces the rate of dark current generation by a factor of 20 or more and thus relaxes CCD cooling requirements to the level where a thermoelectric cooler is sufficient for most applications. Closed cycle cooling systems are becoming more and more popular and they allow operations without daily filling of nitrogen. There are different types of CCD's:

- **Front Illuminated**: used mainly in commercial photography. Peak quantum efficiency as high as 80% can be reached. One of the problems with these devices is the weak fields. Some of the photoelectrons generated in the bulk will be lost, some drift to the neighbouring pixels.
- **Thinned Back Illuminated**: if the starting material is etched, the active layer reaches the back of the detector, and the detector can be back illuminated, improving the collection of the released electrons.
- **Fully Depleted Back Illuminated**: the normal starting material is replaced by high resistant silicon and the detector is thinned but left thicker. The relative large depleted thickness results in good near-infrared response.

- **Frame Transfer and Interline Devices**: the normal imaging area is divided in the imaging and the storage area. The image is first quickly moved to the storage by continuous row transfers, and then clocked out in normal fashion. The first row transfer is fast, taking typically only milliseconds or less. In interline devices each of the active pixels is accompanied with a passive storage pixel. Collected charges are first shifted to the storage columns or lines, which are then clocked out separately.
- **Orthogonal Transfer Devices**: in normal CCDs the charge is clocked down along columns, with channel stops creating potential barriers preventing charge transport in the orthogonal direction. The idea in Orthogonal Transfer CCDs (OTCCD) is to replace channel stops with gates. Charge could be transported in either direction by clocking the gates in certain fashion. Since the charge in OTCCDs can be shifted freely around the detector, it is easier to chain detectors of OTCCDs (mosaics) and use sophisticated amplifier configurations for the readout.
- **L3Vision Devices E2V**: CCD's with special shift registers for electron multiplication. The readout noise is very low and the detector can be read relatively fast.
- **Hybrid Visible Silicon Imagers (HyViSi)**: these detectors combine the best of matrix photodiode detectors with the matrix of CMOS amplifiers. Both are processed separately. The contact between the pixels and CMOS readout amplifiers is done by bump bonding (pixel to pixel). The photodiode can be optimised for the wanted light frequency and manufactured with a fill factor of ~100%. Special coatings can be used for reduced light scattering. Additional benefits are that each of the pixel amplifiers can be optimised much more freely than in the case of CMOS imagers, because obscuring the path of light to the sensitive volume of the silicon is not an issue. These hybrid detectors can in principle have the best of both: the sensitivity of the CCDs and the ease of use of the CMOS detectors. Currently the problem could be the dark current and the cooling system needed to compete with CCD detectors.

To illustrate the current limits of the technology in this branch, the camera of the future Largest Synoptic Survey Telescope (LSST) is considered. The LSST camera will be the largest digital camera ever constructed. Its size of 1.6 meters by 3 meters is roughly equal to that of a small car and it will weigh 2800 kilograms. It is a large-aperture, wide-field optical (0.3-1 μm) imager designed to provide a 3.5 deg FOV with better than 0.2 arcsec sampling. The image surface is flat with a diameter of approximately 64 cm. The detector format will be a mosaic of 16 Mpixel silicon detectors providing a total of approximately 3.2 Gpixels. The camera includes a filter changing mechanism and shutter. It is positioned in the middle of the telescope where cross sectional area is constrained by optical vignetting and heat dissipation must be controlled to limit thermal gradients in the optical beam. The camera will produce data of extremely high quality with minimal downtime and maintenance. CCDs are the baseline science sensors but also hybrid CMOS detectors are pursued as an option for the guide sensors. With 150 connections per sensor and a total of 3024 output ports only 2 s will be needed for the readout [RD-17].

From the analysis of the existing cameras, it results that the choice of the astronomers is the backside illuminated CCD detector, even for very innovative projects like the LSST telescope. The 'standard' size of the detectors is 2kx2k or 4kx4k. The tendency in large mosaic projects is to build modules of two or four CCDs, with common electronics and mechanical support. Electronic connections in mosaics are from the 'back' of the modules. Sophisticated packaging with very high filling factor exists (98%). Cooling can be passive or thermoelectric. Read times vary considerably, because there are different arrangements for readout, different number of readout channels and amplifiers on the chip. Typical data rates for astronomy imaging are 50k-1.5M pixels/s. The noise level depends again on the readout speed, but is in the range 3-10 e-/px. Current and near future astronomy projects do not use monolithic CMOS-detectors or HyViSI hybrids in scientific experiments where quantum efficiency and low noise are important. Hybrid CMOS circuits and CMOS APS detectors are challenging CCDs in low-end and in professional imaging. However, the best choice for astronomy applications is still the back-illuminated CCD. It is nearly perfected, with high quantum efficiency, lowest noise, and by far, lowest dark current. The CCD-detector is also the unanimous choice of the instrument groups developing new devices for the focal plane telescopes in space and on Earth. Compact electronics, sophisticated mechanics, and effective cooling systems for these CCDs will be available. Additional benefits include, that the CCD chips used in these large projects, will be characterized extremely well.

Mount

The telescope mounts are analyzed with respect to the following factors (Table 2):

- Slewing speed
- Pointing accuracy

- Tracking accuracy
- Encoder resolution

The table includes amateur equipment, which does not satisfy the quality required for SSA, but they help to fill the otherwise very scarce dataset: there is not much price information about professional telescope mounts because they are all built with the custom telescope. Therefore, the additional low-end data give extra points used to extrapolate cost estimates. Following mount models are considered: Gaiax (Vixen Optics), Paramount ME Robotic Telescope System (Software Bisque), different RCOS models (RC Optical Systems), and the mount used for the Sloan Digital Sky Survey (SDSS) telescope.

Name	Type	Tracking ["]	Pointing ["]	Slewing [°/s]	Enc. resol. ["]	Cost [Eur]
Vixen Gaiax	g. eq.	5	180	2	-	11000
Paramount ME	g. eq.	<1	10-30	5	0.3	10300
RCOS 3600 GTO	g. eq.	0.5	<60	3	0.05	18 900
RCOS PS EQ fork	f. eq	3	15-20	3	-	-
RCOS EL/AZ gimbal	altaz	1.1	1.7	17	0.002	-
SDSS	altaz	0.165	2	3	0.0072	2010000

Table 2. Accuracy and cost of different mount models. The types are: German equatorial (g. eq.), fork equatorial (f. eq.) and Alt/Az (altaz).

There are of course much more mechanical parameters for the telescope mounts which usually can not be analyzed from the reported parameters, like mechanical flexibility of the mount, absolute accuracy of the angle encoders or periodic errors of the tracking. These values, however, are included in the values of pointing and tracking accuracy that also describe the performance of the telescope control software and especially the quality of the used telescope pointing model. Even though the full seven parameter set, as described by standard pointing model, enables the calculation of pointing simulations, it is quite hard to predict the final telescope performance from these values [RD-18]. The accuracy of the angle encoders can be as fine as 0.3" but the final pointing inaccuracy of the telescope can rise due to mechanical and physical error sources to 10"-30" [RD-19]. In the Sloan Digital Sky Survey (SDSS) telescope, the incremental angle encoder accuracy is ±1" and the read accuracy of the encoders 0.18” before the 25:1 gear reduction, whereas the final pointing accuracy of the telescope is 2" [RD-20].

In general, the length of the telescope tube varies from the half of the aperture diameter (e.g. extreme Cassegrain for space applications) to five times or more the diameter (e.g. classical Schmidt), depending on the focal ratio of the telescope. For Cassegrain optics the typical length from secondary to focal plane is 1/3 of the effective focal length of the telescope. The optical tube length contributes to the rotational inertia of the telescope, which in turn affects the slewing speed. Another effect is the deformation of the tube due to gravitation, which takes effect more strongly in long tubes. The rotational inertia of the telescope depends on the mass distribution of its components. The main masses of the telescope tube are usually situated at the main mirror box and at the secondary mirror support. Modern wide field telescopes can have significant amount of mass also behind the main mirror due to large corrector lenses and needed rigid support systems. The secondary mirror support mass has a strong effect on the rotational inertia. Due to balancing requirements the center of mass of the telescope tube is in general situated at the rotation axis.

From the above considerations it results that the optical tube should possibly be relative short and the suitable mount for the envisaged aperture range and purpose is an Alt/Az mount. The dynamical tresses in the mount are then more symmetrical and thus the azimuth structure can be lighter. In the frame of SSA the telescopes could have an identical mount and light telescopes could be transferred from site to site or positioned more freely. The pointing accuracy 1" is reached only in specific cases, whereas mass produced mounts have pointing precision around 0.5’. The blind pointing accuracy relies on the accuracy of the encoders and on the stability of the encoder setting points at the mount. Incremental encoder without gearing can have divisions of 36’000 per revolution (0.1") with accuracy of ±0.4", while absolute encoder without gearing can have accuracy of ±1". A mount similar to the RCOS EL/AZ Gimbal Fork Alt/Az model seems to be suitable to this task, even though it needs some upscaling to aperture ranges around 1 m.

TELESCOPE COSTS

There are several cost versus telescope aperture diameter approximations. The traditional cost scaling law is [RD-21][RD-22]:

$$\text{cost} \propto D^{2.7}$$

Approximations for older telescopes with heavy monolithic mirrors and heavy equatorial mounts prior to the 1980's yield:

$$\text{cost} \propto D^{2.8}$$

The cost approximation for newer telescopes with lighter monolithic mirrors and ALT-AZ mounts has dropped slightly, scaling to:

$$\text{cost} \propto D^{2.5}$$

In the models proposed for the telescope costs, the OTA, the camera, the mount, and the observatory with the instrumentation and the building are usually considered. Other models taking only into account the OTA costs support other scaling laws with powers smaller than 2. In general the models indicate that telescope components related to surface area (such as polishing mirrors) increase cost as diameter squared while structures such as the mount or dome (related to volume) increase cost as diameter cubed. Thus if the cost of the whole observatory is estimated, values between 2 and 3 are obtained [RD-23]. Furthermore, the contribution of radius of curvature to the OTA cost is not as significant when compared to that of the diameter, since the primary mirror diameter is a stronger cost driver. Note that the radius of curvature may have a different effect in the OTA cost than it would for telescope or observatory. This is because a shorter curvature radius means that the telescope mount and the observatory can be smaller, and hence, this could substantially decrease the overall telescope cost.

Factors to consider for additional cost savings are segmented primary mirrors and arrays of telescopes. For instance, the Keck telescopes (Mauna Kea, HI) use 36 hexagonal segments to form 10 m diameter primary mirrors. The cost reduction might be attributable to the fact that smaller mirror segments are stiffer than large monolithic mirrors and hence may be easier to make, but this is balanced by the need to create stiffness with the support structure. The complex interplay between segment size and learning curve is explained in [RD-23]. In an array of telescopes (frequently referred to as an interferometer or a phased array) images are combined to create the effect of having a larger telescope. For example, the Center for High Angular Resolution Astronomy (CHARA) array (Mt. Wilson Ob., CA) consists of six 1 m duplicate telescopes.

Telescope mount costs approximately as much as the telescope tube and optics because the costs scales according to needed rigidity and according to increased pointing accuracy which both increase with increasing telescope aperture diameter. The angle encoders and the read electronics are the most expensive electronic parts of the mount: the high-end versions for a single mount cost about 20’000 EUR.

As an example, hereinafter the costs of OTA and mount for the SDSS telescope are indicated:

Optics: 2’556 k$
Cast Primary: 635 k$
Purchase Secondary blank: 40 k$
Polish Primary: 1’015 k$
Polish Secondary: 620 k$
Purchase Correctors: 286 k$

Mount: 2’417 k$
Design: 588 k$
Mount Fabrication: 1’286 k$
Mount Installation: 41 k$
Controls: 183 k$
External Wind/Light Baffles: 146 k$
Misc./Unalloc. hardware: 173 k$

Other: 496 k$
Mirror Supports: 60 k$
Internal Light Baffles: 280 k$
Thermal Control Primary: 156 k$

Total: 5469 k$

The costs for the camera depend on the actual detector (e.g. CCD device), on the controller electronics, the cooling system, and related structures. Costs data were taken from different sources, including the costs for the camera of the ZIMLAT telescope in Zimmerwald, the ESASDT telescope on Tenerife, and the CCD MOSAIC cameras at the Kitt Peak National Observatory (Arizona) [RD-24]. The cost of a CCD device only can be estimated to be around 20’000 EUR for a size of 3 cm x 3 cm. The cost increases with the square of the size, i.e. a 6 cm x 6 cm detector costs four times more. This value is essentially characterized by the manufacturing costs. For large sensors the cooling system tends to play a marginal role, whereas a big fraction of the camera price is taken by the controller. The controller electronics costs at least as much as the detector itself. Depending on the size of the detector and on the characteristics, like e.g. number of readout ports, the controller needs to be ad hoc configured, involving development costs in addition to the hardware components. For certain cameras almost at prototype level the development expense can rise up to three times the cost of the only detector. For mosaic detectors, there is a constant initial cost due to a more complex architecture and a slight linear dependence on the number of mosaic pieces. For the analyzed cameras the constant amount is about 300’000 EUR plus on average about 25’000 EUR development cost per mosaic piece. This means that a camera with a mosaic of 8 square detectors with 4 cm x 4 cm would cost about 1 Mio EUR. The mosaic segments alone would cost around 400’000 EUR and the controller 500’000 EUR. The remaining 100’000 EUR could be the fraction due to the cooling circuit and supporting structures. The costs of the development part for the controller, i.e. all non-hardware costs, can be reduced, though not neglected, if

the same camera is produced again or several times: the assembly will always take some effort and for a mosaic camera it will be even worse. Also a serious testing in each phase is needed and sometimes problems are discovered even if the design is just a copy. Probably the same 1 Mio EUR prototype camera would cost the second time about 600k EUR. However, if the camera includes some COTS parts then the price could only drop perhaps by 1/3 or 1/4. But this point is important especially for the Space Surveillance Network where the same sensor system could be used on more than one telescope and on many sites.

Figure 1 shows the cost of the detector and the camera as a function of the detector size. The detector cost given at 12 cm considers a mosaic of four pieces. As prototype are indicated the cameras where a considerable effort in the controller development was put, in order to achieve better performances, e.g. in the readout speed. For sizes bigger than 6-8 cm the costs for the detector only start to be high and the trend curve for prototype controllers almost prohibitive. For larger cameras the reasonable solution is adopting mosaic detectors. The price of a mosaic is elevated due to a more complex architecture, but it scales approximately as the detector costs.

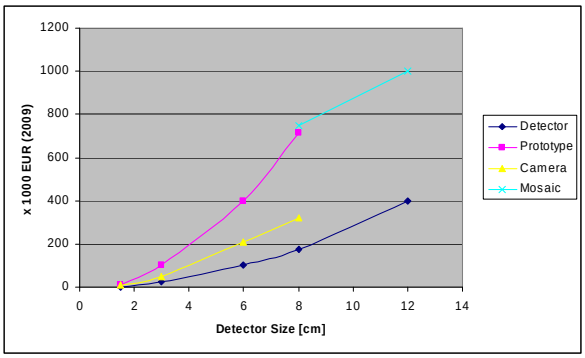

Figure 1. Cost of detector only (blue), low-end (yellow), prototype (violet), and mosaic (light blue) camera, as a function of size.

REQUIREMENTS

According to the given requirements for the optical SSN network, three levels were defined, corresponding to an Enhanced Phase (Level 1), a Full Programmed Phase (Level 2), and a relaxed Phase (Level 3). The different levels apply to two design drivers of the system, namely the limiting size of the object to be detected and the timeliness for detecting particular events (e.g. fragmentations, maneuvers). The limiting size for Level 1 is 50 cm in GEO and 30 cm in MEO. For Level 2, 70 cm (GEO) and 50 cm (MEO), and for Level 3, 100 cm and 80 cm for GEO and MEO, respectively. Figure 2 illustrates the dependence of the magnitude on the object diameter and phase angle with a distance of 25000 km for the MEO region. For the calculations a spherical shape and a Bond albedo of 0.1 are assumed. From the diagram magnitudes around 17-18 mag, 16-17 mag, and 15-16 mag for the three levels are found. For the phase angle a reasonable limit around 70-80 deg is assumed. The magnitudes for GEO objects were calculated in a similar way. Table 3 summarizes the object sizes and magnitudes for the different levels.

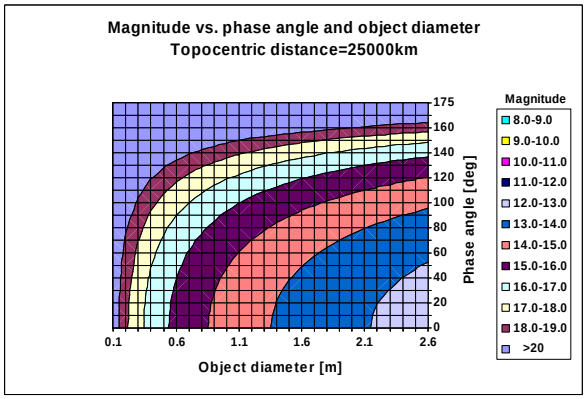

Figure 2. Magnitude as a function of phase angle and diameter for objects in MEO.

Level	GEO	MEO	Mag. GEO	Mag. MEO
Level 1	50 cm	30 cm	17-18	17-18
Level 2	70 cm	50 cm	16.5-17.5	16-17
Level 3	100 cm	80 cm	16-17	15-16

Table 3. Object sizes and magnitudes for the three levels.

In Figure 3 the SNR as a function of the sky background and the magnitude is shown for a 1.2 m aperture. The assumed object velocity of 36”/s represents objects on MEO orbits, with about 2.5 revolutions per day. The model used for the calculations is explained in [RD-25]. The following values are assumed:

- Integration time: 2 s
- Optical transmission: 65%
- Quantum Efficiency: 80%
- Readout noise: 10 e^-/px
- Dark Current: 0.2 e^-/(s*px)
- Point Spread Function (PSF) size: 15 µm

The calculations assume that an ideal detection algorithm recognizes the object (streak) on the exposure frames. Then the indicated SNR threshold of 4, based on the results of simulations performed in the SSA

study [RD-26], is a reasonable value for detection within the required accuracy. The model assumes perfect visibility conditions and for the evaluation of the different aperture diameters a limiting sky background of 18 mag/arcsec^2 is taken into account. This implies that no Milky Way appears in the pointed direction and that the effect of the moon light is negligible. Some of the parameters assumed for the calculations are only provisional at this stage and need to be refined in further iterations. A focal ratio f/2 was used to compute the diagram and it has to be noted that the detection varies of about 0.5 mag between f/1 and f/2, which is not so relevant.

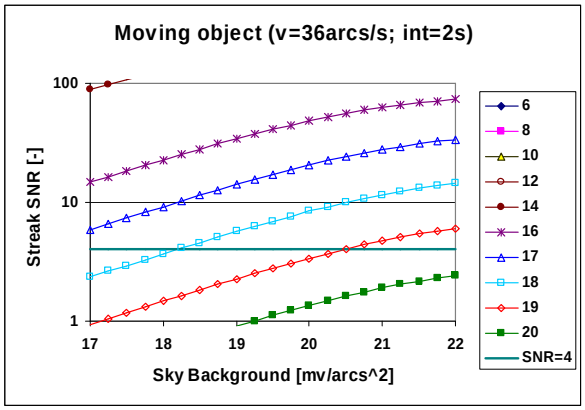

Figure 3. SNR as a function of sky background and magnitude for 1.2 m aperture diameter

In a similary way the SNR for other aperture diameters and for GEO objects was calculated. It results that the apertures needed for Level 1, 2, and 3 in GEO are 0.9 m, 0.7 m, and 0.5 m, while for MEO, 1.2 m, 0.8 m, and 0.4 m, respectively. This means the following requirements for a common GEO-MEO telescope:

- Level 1: 1.2 m aperture
- Level 2: 0.8 m aperture
- Level 3: 0.5 m aperture

PRELIMINARY DESIGN

Starting from the given apertures, different trade-offs in terms of requirements, telescope capabilities, and costs need to be examined. The problem can be approached in a pragmatic way by prioritizing the most relevant dependences. The scheme shown in Figure 4 proposes a possible approach, starting with the limiting object size. On the left (green) are the requirements, in the center (blue) the telescope parameters, on the right (brown) the costs, and at every level of the scheme a possible trade-off needs to be examined.

As seen previously the limiting size, in first approximation, determines the aperture diameter of the telescope. However, the aperture is strictly related to the focal ratio F = f / D (also indicated f/#), where f is the focal length and D the diameter. From the previous analysis of the costs it results that for larger telescopes the focal ratio is not the relevant factor. On the other hand, it is preferable to have a small focal ratio, hence a short focal length, for wide-field applications. In the subsequent analysis values of f/1.5 – f/2 will be assumed.

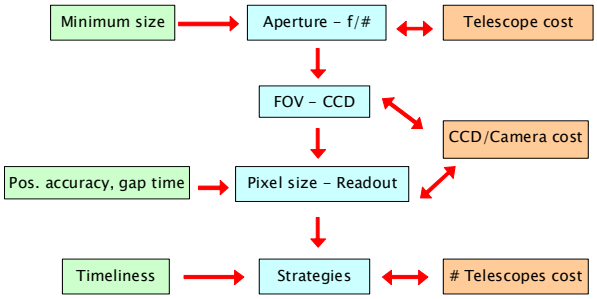

Figure 4. Approach for the definition of the telescope parameters (blue) with the requirements (green) and the costs (brown).

In the second step of Figure 4 to determine the size of the camera, the FOV, related to detector size s through FOV = s / f, needs to be analyzed. For SSA applications it is desirable to have a large FOV, but this implies larger cameras with higher costs. In Figure 5 the cost dependence on the FOV is displayed for different telescope apertures, assuming a focal ratio f/1.5. The FOV is related to the detector size s by the formula FOV = s / (F*D).

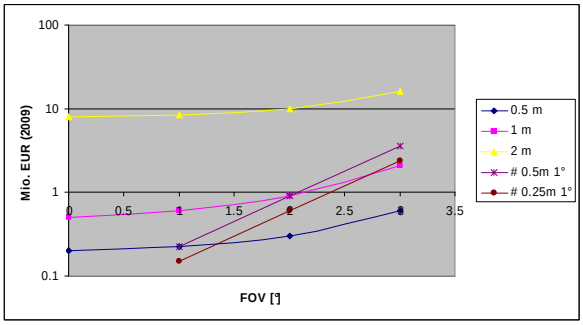

Figure 5. Cost as a function of FOV for different apertures and focal ratio f/1.5. In brown and violet the FOV is covered by multiple 1 deg FOV telescopes.

For the camera, the costs of monolithic detectors with aforementioned prototype controllers are adopted. The brown and violet plots refer to telescopes with 1 deg FOV value: the cost is calculated taking multiple identical telescopes with this value in order to cover an equivalent total FOV. Up to 2 deg FOV the configuration of 0.25 m and 0.5 m telescopes is still

cheaper than the 1 m telescope. Above 2 deg FOV the single 1 m telescope starts to be more convenient. However, at same telescope sensitivity (same aperture) the single telescope is always less expensive. This means that it is preferable to strive for larger FOV's given a certain aperture, with the drawback of more complex optical designs.

The third step takes as input the accuracy in the position determination of the observed object and the gap time between two exposures. These two parameters are strictly related to the capability of the camera. The detection accuracy depends on the pixel scale, which in turn depends on aperture and pixel size. Figure 6 shows this dependence using a reasonable pixel size of 15 μm and a focal ratio f/1.5. According to [RD-26] the centroiding accuracy for similar telescope parameters is about 1/10 of the pixel size. Taking into account additional errors in the astrometric determination, an upper limit of 0.5 pixels in the position accuracy can be relied on. This results in about 1" accuracy for 1 m aperture and 2"/px pixel scale. Smaller pixels do not bring additional accuracy since usually the PSF is already in the order of 10 μm. The gap time between two exposures depends on the slew velocity of the mount and on the readout time of the camera. In this case, as for the pixel size, the trade-off is clear: one needs the fastest possible readout, although this might slightly increase the readout noise. Technology for readout time of about 3 s is today available and a slew time smaller than 3 s per step is feasible.

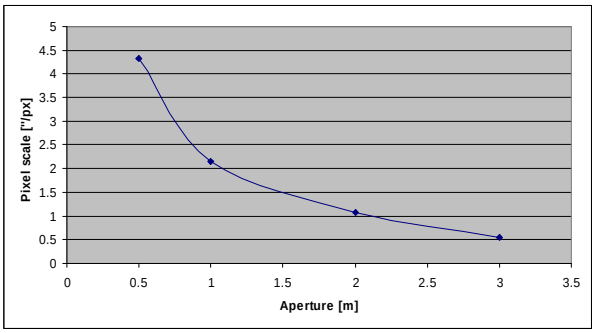

Figure 6. Pixel scale as a function of the aperture. Pixel size 15 μm and focal ratio f/1.5.

The last point concerns the timeliness for specific events. Once the potential FOV is defined, this aspect is independent from the characteristic of the optical assembly and depends only on the observation strategy. According to the strategy the number of necessary telescopes with a given FOV is determined.

Based on the previous considerations the telescopes grid in Table 4 is proposed. For the Level 1 telescope, with 1.2 m diameter, a FOV of 4 deg sounds a reasonable choice. Alternatively, a second, cheaper, less ambitious version is proposed for Level 1 with only 2 deg FOV. For the less demanding Level 2 and Level 3 the following values are proposed together with a cheaper version: 0.8 m / 4.5 deg, 0.8 m / 2.5 deg, 0.5 m / 5 deg, and 0.5 m / 3 deg. The 0.5 m / 3 deg design is already close to the COTS available telescopes. The cost estimate for the 1.2 m / 4 deg, based on the previous results, foresees about 1.5 Mio EUR for OTA and mount, and 1-1.5 Mio EUR for the camera. In this case the camera cost is really an additional cost not included in the aforementioned cost models, since its 16 cm size makes it extraordinary. Further costs could arise from the development of corrector designs, where the research effort can be almost arbitrarily prolonged to reach an optimum. The latter costs are also difficult to estimate because relative new wide-field correctors are scarce documented. As an example of costs with a long design period, the Skymapper telescope [RD-27] at the Siding Spring Observatory with 1.3 m diameter, f/4.8, and 2.37 deg FOV will cost about 6.2 Mio EUR plus 1.5 Mio EUR for the camera.

Lev.	Aper.	FOV	Detec.	Pix. Sc.	EUR
L1	1.2 m	4°	16 cm	1"/px	3-4 Mio
L1*	1.2 m	2°	8 cm	1"/px	1.5 Mio
L2	0.8 m	4.5°	10 cm	2"/px	1-1.5 Mio
L2*	0.8 m	2.5°	6 cm	2"/px	700-800k
L3	0.5 m	5°	8 cm	2"/px	500-700 k
L3*	0.5 m	3°	4 cm	2"/px	200 k

Table 4. Telescope parameters and costs for the three levels (L1, L2, L3). The symbol * denotes the cheaper version.

CONCLUSIONS

The analysis of the existing telescopes shows that in general it is hard to reach wide FOV for large apertures. The difficulties are either complicated necessary designs, or manufacture limitations to reach desired aperture range over 1 m. The most promising designs base on field-corrected RC or super-RC systems, reaching 4 deg FOV or more with 1.2 m aperture diameter. Regarding the cameras, it results that the choice of the astronomers is the backside illuminated CCD detector, even for very innovative projects like the LSST telescope. The 'standard' size of the detectors is 2kx2k or 4kx4k. The tendency in large mosaic projects is to build modules of two or four CCDs, with common electronics and mechanical support. Read times vary considerably, because there are different arrangements for readout, different number of readout channels and

amplifiers on the chip. Typical data rates for astronomy imaging are 50k-1.5M pixels/s. The noise level depends again on the readout speed, but is in the range 3-10 e-. The suitable mount for the envisaged aperture range and purpose is an Alt/Az mount. The dynamical tresses in the mount are then more symmetrical and thus the azimuth structure can be lighter. The blind pointing accuracy relies on the accuracy of the encoders and on the stability of the encoder setting points at the mount. Incremental encoder without gearing can have divisions of 36'000 per revolution (0.1") with accuracy of ±0.4", while absolute encoder without gearing can have accuracy of ±1".

In the models proposed for the telescope costs, the OTA, the mount, and the observatory with the instrumentation and the building are considered: the dependence indicates a power law with an exponent between 2 and 3. The contribution of radius of curvature to the OTA cost is not as significant when compared to that of the diameter. The telescope mount costs approximately as much as the telescope tube and optics because the costs scales according to needed rigidity and pointing accuracy. The costs for the camera mostly depend on the actual detector and on the controller electronics. The detector cost increases with the square of the size and is essentially characterized by the manufacturing process. The controller electronics costs at least as much as the detector itself. Depending on the size of the detector and on the characteristics, development costs in addition to the hardware components are involved. For mosaic detectors, there is a constant initial cost due to a more complex architecture and a slight linear dependence on the number of mosaic pieces. The costs of the development part for the controller, i.e. all non-hardware costs, can be substantially reduced if the same camera is produced again or several times.

According to the SSA requirements three different levels were defined with the following apertures: 1.2 m, 0.8 m, 0.5 m. The aperture is strictly related to the focal ratio and from the analysis of the costs it results that for larger telescopes the focal ratio is not the relevant factor. However, it is preferable to have a small focal ratio for wide-field applications: values of f/1.5 – f/2 are assumed. For SSA applications it is desirable to have a large FOV, but this implies larger cameras with higher costs. The analysis shows that at same telescope sensitivity (same aperture) the single telescope is always less expensive than multiple telescopes with a smaller FOV. It is preferable to strive for larger FOV's given a certain aperture, with the drawback of more complex optical designs.

The accuracy in the position determination of the observed object and the gap time between two exposures are strictly related to the capability of the camera. The detection accuracy depends on the pixel scale, which in turn depends on aperture and pixel size. Calculations indicate 1" accuracy for 1 m aperture and 2"/px pixel scale. The gap time between two exposures depends on the slew velocity of the mount and on the readout time of the camera. Technology for readout time of about 3 s is today available and a slew time smaller than 3 s per step is feasible.

For the Level 1 telescope, with 1.2 m diameter, a FOV of 4 deg sounds a reasonable choice. Alternatively, a second, cheaper, less ambitious version is proposed for Level 1 with only 2 deg FOV. For the less demanding Level 2 and Level 3 the following values are proposed together with a cheaper version: 0.8 m / 4.5 deg, 0.8 m / 2.5 deg, 0.5 m / 5 deg, and 0.5 m / 3 deg. The cost estimate for the 1.2 m / 4 deg, based on the previous results, foresees about 1.5 Mio EUR for OTA and mount, and 1-1.5 Mio EUR for the camera. Further costs could arise from the development of corrector designs, where the research effort can be almost arbitrarily prolonged to reach an optimum.

ACKNOWLEDGEMENTS

This work was done under ESA/ESOC contract 22738/09/D/HK.

REFERENCES

[RD-1] http://pan-starrs.ifa.hawaii.edu/public/design-features/telescopes.html

[RD-2] http://www.lsst.org/lsst

[RD-3] http://www.lpl.arizona.edu/css

[RD-4] http://www.astro.uu.se/history/USS.html

[RD-5] http://www.mso.anu.edu.au/observing/telescopes/40inch.php

[RD-6] http://www.lpl.arizona.edu/css/css_facilities.html

[RD-7] www.aiaa.org/Spaceops2002Archive/papers/SpaceOps02-P-T2-01.pdf

[RD-8] www.oosa.unvienna.org/pdf/pres/stsc2006/tech-10.pdf

[RD-9] http://cas.sdss.org/dr7/en/sdss/telescope/telescope.asp

[RD-10] http://tarot.obs-hp.fr/infos

[RD-11] www.oosa.unvienna.org/pdf/pres/stsc2006/tech-10.pdf

[RD-12] http://www.aiub.unibe.ch/content/zimmerwald/the_zimlat_telescope/index_eng.html

[RD-13] http://esamultimedia.esa.int/multimedia/esoc/opsg/opsgforum_esa__optical_ground_station_20080118.pdf

[RD-14] http://www.telescope.org/infopage.php?title=Tenerife_Telescope_Hardware#Galaxy

[RD-15] Ackermann, M.R., McGraw, J.T., Zimmer, P.C., Williams, T., "The unique optical design of the NESSI Survey Telescope", AMOS Conference, Maui, Hawaii, 2006

[RD-16] McGraw, J.T., Ackermann, M.R., A 1.2m deployable, transportable Space Surveillance Telescope designed to meet AF Space Situational Awareness Needs", AMOS Conference, Maui, Hawaii, 2007

[RD-17] http://www.lsst.org/lsst/science/concept_camera

[RD-18] Wallace, P.T., Tritton, K.P., "Alignment, pointing accuracy and field rotation of the UK 1.2-m Schmidt Telescope", Monthly notices of the Royal astronomical society, vol. 189, p.115-122, 1979

[RD-19] https://www.bisque.com/help/paramountme/performance_specifications.htm

[RD-20] Rivetta, C.H., Briegel, C., Czarapata, P., "Motion control design of the SDSS 2.5 mts telescope", Proc. SPIE Vol. 4004, p. 212-221, Telescope Structures, Enclosures, Controls, Assembly/Integration/Validation, and Commissioning, eds. Sebring T. & Andersen T., 2000

[RD-21] Larry M. Stepp, Larry G. Daggert, and Paul E. Gillett, "Estimating the cost of extremely large telescopes", Proc. SPIE 4840, p. 309, 2003

[RD-22] Gerard T. van Belle, Aden B. Meinel, and Marjorie P. Meinel, "The scaling relationship between telescope cost and aperture size for very large telescopes", Proc. SPIE 5489, p. 563, 2004

[RD-23] Stahl, H.P., Rowell, G.H., Reese, G., Byberg, A., "Multivariable parametric cost model for ground optical telescope assembly", Optical Engineering 44 (8), 2005

[RD-24] Larry M. Stepp, Larry G. Daggert, and Paul E. Gillett, "Estimating the cost of extremely large telescopes", Proc. SPIE 4840, p. 309, 2003

[RD-25] Schildknecht, T., "Optical Astrometry of Fast Moving Objects using CCD detectors", Geodätisch-geophysikalische Arbeiten in der Schweiz, no. 49, 1994

[RD-26] Donath, T., Schildknecht, T., Sanchez, N., Bunte, K., Alonso Madero, F., Dorn, C., Dick, J., Martinot, V., Piemontese, M., "Proof of Concept for Enabling Technologies for Space Surveillance", ESA AO/1-5354/07/NL/ST, Final Report, ONERA, 2010

[RD-27] http://rsaa.anu.edu.au/skymapper/index.php